

Contribution from the Christopher Ingold Laboratories, University College London, 20 Gordon Street, London WC1H 0AJ, England, and Department of Chemistry, Birkbeck College, Gordon House, 29 Gordon Square, London WC1E 6BT, England

Infrared, Raman, Resonance Raman, and Excitation Profile Studies of $\text{Rh}_2(\text{O}_2\text{CCH}_3)_4(\text{PPh}_3)_2$ and Its ^{18}O and CD_3 Isotopomers

Robin J. H. Clark*[†] and Andrew J. Hempleman^{†,‡}

Received November 4, 1987

The resonance Raman spectra of $\text{Rh}_2(\text{O}_2\text{CCH}_3)_4(\text{PPh}_3)_2$ and its ^{18}O and CD_3 isotopomers have been recorded at ca. 80 K. A band at 289 cm^{-1} , denoted ν_1 , is assigned to $\nu(\text{Rh-Rh})$ and is the dominant progression-forming mode. This band also forms combinations with bands attributable to the tetraacetate cage, such as $\nu(\text{Rh-O})$ and $\delta(\text{OCO})$, as well as with those of the axial PPh_3 ligands. Excitation profiles of $\nu(\text{Rh-Rh})$ and several other bands are shown to maximize under the 376-nm electronic absorption band, which, by way of Raman band depolarization ratio measurements, is assigned to an axial (z) polarized transition terminating in $\sigma^*(\text{RhRh})$. Bands assigned to $\nu(\text{Rh-O})$ are shown to be dependent on both ^{18}O and CD_3 substitution. For $\text{Rh}_2(\text{O}_2\text{CCH}_3)_4(\text{PPh}_3)_2$, Raman spectra obtained with 514.5-nm excitation are also discussed. FTIR spectra ($3500\text{--}40\text{ cm}^{-1}$) of $\text{Rh}_2(\text{O}_2\text{CCH}_3)_4(\text{PPh}_3)_2$ and its ^{18}O and CD_3 isotopomers are also presented and assigned. The results provide a firm basis for making vibrational band assignments for other dimetal tetracarboxylates.

Introduction

In an earlier communication the longstanding controversy regarding the assignment of $\nu(\text{RhRh})$ in dirhodium tetracarboxylates was discussed and resolved, in the case of $\text{Rh}_2(\text{O}_2\text{CCH}_3)_4(\text{PPh}_3)_2$, in favor of the band at 289 cm^{-1} detected in the resonance Raman spectrum.¹ This paper reports more fully on the assignment of the Raman and resonance Raman spectra of $\text{Rh}_2(\text{O}_2\text{CCH}_3)_4(\text{PPh}_3)_2$ and its ^{18}O and CD_3 isotopomers. In particular, the wavelength range of the previously reported resonance Raman spectra has been extended, Raman band excitation profiles have been plotted, and detailed infrared spectra ($3500\text{--}40\text{ cm}^{-1}$) are included. This comprehensive study now puts the assignment of $\nu(\text{Rh-Rh})$, $\nu(\text{Rh-O})$, and other skeletal bands on a firm basis and opens the way to clarifying the vibrational band assignments for other dimetal tetracarboxylates.

Experimental Section

Complexes. $\text{Rh}_2(\text{O}_2\text{CCH}_3)_4(\text{PPh}_3)_2$ was prepared by the dropwise addition of a saturated methanolic solution of PPh_3 to a methanolic solution of $\text{Rh}_2(\text{O}_2\text{CCH}_3)_4$. The resultant orange precipitate was recrystallized from dichloromethane. Anal. Calcd for $\text{Rh}_2(\text{O}_2\text{CCH}_3)_4(\text{PPh}_3)_2$: 54.7, C; 4.38, H; 6.41, P. Found: 54.5, C; 4.39, H; 6.50, P. Samples of ^{18}O - and CD_3 -substituted $\text{Rh}_2(\text{O}_2\text{CCH}_3)_4$ were prepared as described previously.¹ Acetic- d_3 acid (99.6% D) was obtained from Aldrich Chemical Co., Inc. Acetic acid (78.5 atom % ^{18}O) was obtained from Miles-Yeda Ltd.

Instrumentation. Raman spectra were recorded with a Spex 14018 (R6) spectrometer, in the double-monochromator mode, in conjunction with Coherent CR 3000 K and CR 12 lasers. The Raman spectra with $\lambda_0 = 514.5\text{ nm}$ were also obtained in the triple-monochromator mode for the low-wavenumber region ($<400\text{ cm}^{-1}$). Raman samples were held as pressed KCl disks at ca. 80 K using a liquid-nitrogen-cooled cell. Infrared spectra were recorded at ca. 80 K as KCl disks ($3500\text{--}500\text{ cm}^{-1}$) and as pressed wax disks ($660\text{--}40\text{ cm}^{-1}$) at a spectral resolution of 1 cm^{-1} with a Bruker 113 V interferometer. The wax disks were prepared by adding the complex to the melted wax (mp $49\text{ }^\circ\text{C}$, BDH), and then, as the wax was allowed to solidify, vacuum was applied in order to remove any air present in the wax (since this has been found to give rise to high backgrounds). The resulting solid was then pressed between Teflon plates, one of which was wedged at an angle of 1° . Overlap between the mid- and far-infrared regions allowed matching of band intensities, which are quoted on an arbitrary absorbance scale of $\text{vw} < 0.02$, $\text{w} = 0.02\text{--}0.2$, $\text{m} = 0.2\text{--}0.6$, $\text{s} = 0.6\text{--}0.9$, and $\text{vs} > 0.9$; $\text{br} = \text{broad}$, $\text{sh} = \text{shoulder}$.

Results and Discussion

The resonance Raman spectrum of $\text{Rh}_2(\text{O}_2\text{CCH}_3)_4(\text{PPh}_3)_2$ obtained with 356.4-nm excitation is shown in Figure 1, and the band positions are listed in Table I. There are no strong bands in the $170\text{--}150\text{ cm}^{-1}$ region; in fact there are no bands observed below 289 cm^{-1} . The very strong band at 289 cm^{-1} , denoted ν_1 ,

Table I. Wavenumbers/ cm^{-1} of Bands Observed in the Resonance Raman Spectrum^a of $[\text{Rh}_2(\text{O}_2\text{CCH}_3)_4(\text{PPh}_3)_2]$ at ca. 80 K

| $\bar{\nu}$ | assignt | $\bar{\nu}$ | assignt |
|-------------|----------------------------|-------------|-------------------------------------|
| 289 vs | $\nu_1, \nu(\text{Rh-Rh})$ | 1001 w | p-ring |
| 305 vw | $\nu(\text{Rh-O})$ | 1012 vw | $\nu_1 + \delta(\text{OCO})$ |
| 320 vw | $\nu(\text{Rh-O})$ | 1038 vw | $2\nu_3$ |
| 338 m | $\nu_2, \nu(\text{Rh-O})$ | 1072 vw | d $\beta(\text{C-H})$ |
| 407 vw | w $\phi(\text{C-C})$ | 1099 w | q X-sens |
| 421 vw | } t X-sens | 1148 vw, sh | $\nu_1 + \nu_2 + \nu_3$ |
| 439 vw | | 1154 vw | $4\nu_1$ |
| 450 vw | | 1175 vw | |
| 521 m | ν_3, γ X-sens | 1186 vw | a $\beta(\text{C-H})$ |
| 578 m | $2\nu_1$ | 1202 vw | $3\nu_1 + \nu_2$ |
| 595 vw | $\nu_1 + 305$ | 1252 vw | $2\nu_1 + 2\nu_2$ |
| 610 vw | $\nu_1 + 320$ | 1269 vw | } e $\beta(\text{C-H})$ |
| 627 m | $\nu_1 + \nu_2$ | 1280 vw | |
| 641 vw | | 1290 vw | $\nu_1 + \text{p-ring}$ |
| 675 vw, br | $2\nu_2$ | 1389 vw | $\nu_1 + \text{q X-sens}$ |
| 688 vw | r X-sens | 1437 vw, br | $\nu_2 + \text{q X-sens}$ |
| 725 vw | $\delta(\text{OCO})$ | 1483 vw, br | m $\nu(\text{C-C})$ |
| 746 vw | f $\gamma(\text{C-H})$ | 1550 vw | |
| 809 w | $\nu_1 + \nu_3$ | 1557 vw | |
| 860 vw | $\nu_2 + \nu_3$ | 1571 vw | l $\nu(\text{C-C})$ |
| 866 w | $3\nu_1$ | 1588 w | k $\nu(\text{C-C})$ |
| 881 vw | $2\nu_1 + 305$ | 1617 vw, br | $2\nu_1 + 2\nu_3$ |
| 915 w | $2\nu_1 + \nu_2$ | 1676 vw | $2\nu_1 + \text{q X-sens}$ |
| 932 vw | | 1724 vw, br | $\nu_1 + \nu_2 + \text{q X-sens}$ |
| 963 vw | $\nu_1 + 2\nu_2$ | 1771 vw, br | $\nu_1 + \text{m } \nu(\text{C-C})$ |
| 976 vw | h $\gamma(\text{C-H})$ | 1877 vw | $\nu_1 + \text{k } \nu(\text{C-C})$ |

^a 356.4-nm excitation.

displays an overtone progression up to $4\nu_1$ and forms combinations with several other bands.

The Raman spectrum obtained with 514.5-nm excitation is shown in Figure 2, and the band wavenumbers are listed in Table II. Again, the 289 cm^{-1} band is the strongest, but the overtone and combination bands shown in the 356.4-nm spectrum are no longer apparent apart from a very weak band at 579 cm^{-1} , which may be $2\nu_1$.

There are no bands due to triphenylphosphine in the $400\text{--}280\text{ cm}^{-1}$ region;² hence, bands in this region must be attributable to the tetraacetate cage itself. Bands attributable to $\nu(\text{M-O})$ carboxylate modes are expected in this region; however, the absence of any strong bands in the $170\text{--}150\text{ cm}^{-1}$ region of both the resonance Raman and Raman spectra suggests that $\nu(\text{Rh-Rh})$ must lie at higher wavenumber than this. In the reported resonance Raman spectra of dimetal tetracarboxylates, it is $\nu(\text{M-M})$ that forms the longest progression, although in a few cases, e.g.

* To whom correspondence should be addressed.

[†] University College London.

[‡] Birkbeck College.

(1) Clark, R. J. H.; Hempleman, A. J.; Flint, C. D. *J. Am. Chem. Soc.* **1986**, *108*, 518.

(2) Clark, R. J. H.; Flint, C. D.; Hempleman, A. J. *Spectrochim. Acta, Part A* **1987**, *43A*, 805.

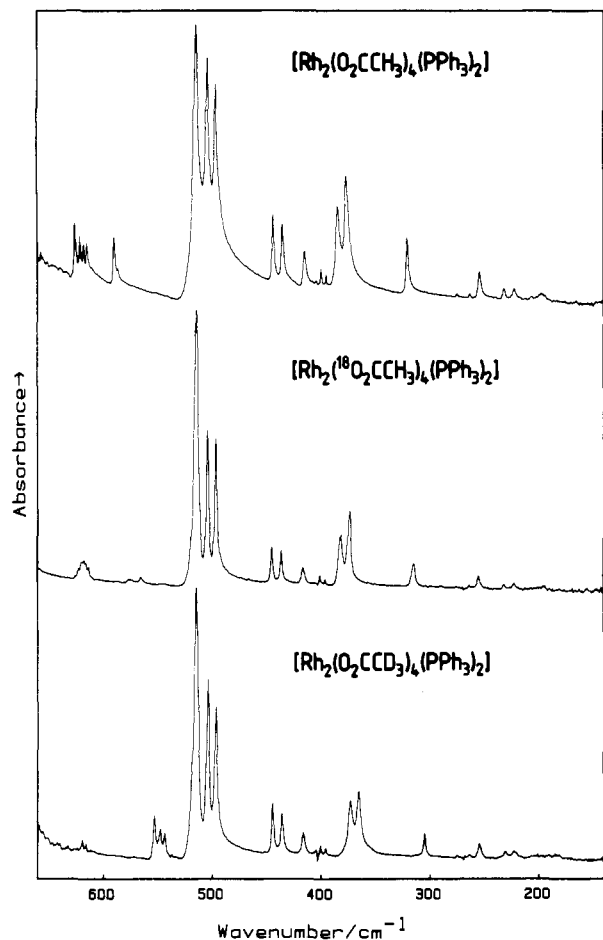


Figure 3. FTIR spectra (660–140 cm⁻¹) of Rh₂(O₂CCH₃)₄(PPh₃)₂, Rh₂(¹⁸O₂CCH₃)₄(PPh₃)₂, and Rh₂(O₂CCD₃)₄(PPh₃)₂ as wax disks at ca. 80 K.

the fact that the 372-cm⁻¹ band appears asymmetric on the low-wavenumber side and therefore may consist of more than one component. Upon ¹⁸O substitution these bands have shifted by differing amounts, resulting in the appearance of a clearly resolved doublet.

Since ν_2 shows such a large sensitivity to deuteration of the methyl group, the contribution of the methyl group symmetry coordinate to the ν_2 normal coordinate must be large. This was also found to be the case for Mo₂(O₂CCH₃)₄, for which the ratio of the ν_2 band wavenumbers Mo₂(O₂CCD₃)₄/Mo₂(O₂CCH₃)₄ is 0.97;^{5,6} cf. for the ν_2 band of Rh₂(O₂CCH₃)₄(PPh₃)₂, where this ratio is 0.96. Quite clearly the description $\nu(\text{Rh-O})$ is an approximate one.

Two other very weak bands are observed in this region at 320 and 305 cm⁻¹, which shift upon ¹⁸O substitution to 314 and 302 cm⁻¹, respectively, and are also assigned to $\nu(\text{Rh-O})$. Their intensities compared to that of ν_2 in the resonance Raman spectrum (Figure 1) are lower than that observed in off-resonance conditions (Figure 2) suggesting that, unlike ν_2 , they are attributable to non totally symmetric $\nu(\text{Rh-O})$ modes. Upon deuteration only the highest component is observed, occurring at 307 cm⁻¹, the lower band presumably being obscured by $\nu(\text{Rh-Rh})$.

Assignment of the corresponding infrared-active $\nu(\text{Rh-O})$ bands is also simplified by the absence of any bands due to triphenylphosphine in the 400–300-cm⁻¹ region.² Infrared-active $\nu(\text{M-O})$ bands in tetraacetate compounds appear at higher wavenumber than their Raman counterparts; cf. the observations for Mo₂(O₂CCH₃)₄. In the infrared spectrum of Mo₂(O₂CCH₃)₄, bands at 373, 353, 342, and 311 cm⁻¹ are assigned to $\nu(\text{Mo-O})$, shifting to 363, 343, 321, and 285 cm⁻¹, respectively, upon deuteration.⁶ By comparison, bands at 385, 377, and 321 cm⁻¹ in the infrared spectrum of Rh₂(O₂CCH₃)₄(PPh₃)₂ (Figure 3) are assigned to $\nu(\text{Rh-O})$. Their relative shifts upon ¹⁸O and deuterium substi-

Table III. Wavenumbers/cm⁻¹ of Bands Observed in the Resonance Raman Spectrum^a of [Rh₂(¹⁸O₂CCH₃)₄(PPh₃)₂] at ca. 80 K

| $\tilde{\nu}$ | assignt | $\tilde{\nu}$ | assignt |
|---------------|----------------------------|---------------|---|
| 289 vs | $\nu_1, \nu(\text{Rh-Rh})$ | 1031 vw | b $\beta(\text{C-H})$ |
| 302 vw | $\nu(\text{Rh-O})$ | 1040 vw | 2 ν_3 |
| 314 vw | $\nu(\text{Rh-O})$ | 1074 vw | d $\beta(\text{C-H})$ |
| 332 m | $\nu_2, \nu(\text{Rh-O})$ | 1100 w | q X-sens |
| 406 vw | w $\phi(\text{C-C})$ | 1127 vw | |
| 422 vw | | 1140 vw | $\nu_1 + \nu_2 + \nu_3$ |
| 439 vw | t X-sens | 1152 vw, sh | 4 ν_1 |
| 449 vw | | 1157 vw, sh | c $\beta(\text{C-H})$ |
| 520 m | ν_3, y X-sens | 1186 vw | a $\beta(\text{C-H})$ |
| 577 m | 2 ν_1 | 1195 vw | 3 $\nu_1 + \nu_2$ |
| 591 vw | $\nu_1 + 302$ | 1238 vw, br | 2 $\nu_1 + 2\nu_2$ |
| 602 vw | $\nu_1 + 314$ | 1269 vw | e $\beta(\text{C-H})$ |
| 620 m | $\nu_1 + \nu_2$ | 1280 vw | |
| 663 vw, br | 2 ν_2 | 1290 vw | $\nu_1 + \text{p-ring}$ |
| 688 vw | r X-sens | 1329 vw | $\nu_1 + 2\nu_3$ or $\nu_2 + \text{p-ring}$ |
| 706 vw | $\delta(\text{OCO})$ | 1389 vw | $\nu_1 + q$ X-sens |
| 710 vw, sh | | 1434 vw, br | $\nu_2 + q$ X-sens |
| 715 vw | | 1482 vw, br | m $\nu(\text{C-C})$ |
| 746 vw | f $\gamma(\text{C-H})$ | 1523 vw, br | |
| 753 vw | | 1558 vw | |
| 759 vw | | 1571 vw | l $\nu(\text{C-C})$ |
| 809 w | $\nu_1 + \nu_3$ | 1588 w | k $\nu(\text{C-C})$ |
| 853 vw | $\nu_2 + \nu_3$ | 1620 vw, br | 2 $\nu_1 + 2\nu_3$ |
| 864 w | 3 ν_1 | 1676 vw | 2 $\nu_1 + q$ X-sens |
| 908 w | 2 $\nu_1 + \nu_2$ | 1721 vw, br | $\nu_1 + \nu_2 + q$ X-sens |
| 949 vw, br | $\nu_1 + 2\nu_2$ | 1769 vw, br | $\nu_1 + m$ $\nu(\text{C-C})$ |
| 975 vw | h $\gamma(\text{C-H})$ | 1807 vw, br | |
| 979 vw, sh | $\nu_1 + r$ X-sens | 1877 vw | $\nu_1 + k$ $\nu(\text{C-C})$ |
| 1001 w | p-ring | 1919 vw | $\nu_2 + k$ $\nu(\text{C-C})$ |

^a356.4-nm excitation.

tution are 3 and ca. 12 cm⁻¹ for the uppermost two bands, respectively, and 6 and 16 cm⁻¹, respectively, for the lowest wavenumber bands. The relative shifts upon deuteration are similar to those observed for Mo₂(O₂CCH₃)₄,⁶ i.e., the two uppermost bands shift by less than the lower bands. The observation of three infrared-active bands attributable to $\nu(\text{Rh-O})$ is in contradiction to the predictions of the M₂(O₂CC)₄ model.⁶ Like Mo₂(O₂CC-H₃)₄,¹¹ Rh₂(O₂CCH₃)₄(PPh₃)₂⁸ only possesses one molecule per unit cell, and therefore band splitting cannot arise from factor group coupling but must be due to the low site symmetry, C₂, in the crystal.

The Raman spectrum obtained with 514.5-nm excitation (off-resonance) displays no overtone progressions or combination band involving $\nu(\text{Rh-Rh})$ (Figure 2) although there may be a number of very weak combinations involving $\nu(\text{Rh-O})$. Unlike the Raman spectrum obtained for Mo₂(O₂CCH₃)₄ with 514.5-nm excitation,⁶ in which bands attributable to the acetate group are clearly observed, the spectrum for Rh₂(O₂CCH₃)₄(PPh₃)₂ is dominated by $\nu(\text{Rh-Rh})$. Thus the 514.5-nm spectrum is better described as a preresonance Raman spectrum, in which different bands are detected as compared to the resonance Raman spectrum; however, most of these appear to be due to the axial PPh₃ ligands, and assignment of the acetate group vibrations has to be taken from the infrared spectrum. This is not straightforward owing to overlap with bands due to the axial PPh₃ ligands. The majority of the PPh₃ bands would not be expected to shift upon coordination owing to the close structural similarity between the free and coordinated ligands.⁸

The PPh₃ bands expected to shift upon coordination would be those involving large phosphorus amplitudes, namely, the six X-sensitive vibrations, q, r, y, t, u, and x (Whiffen's nomenclature).¹² For PPh₃² these occur in the overall infrared and Raman ranges 1098–1087, 683, 515–491, 434–410, 274–247, and 214–188 cm⁻¹, respectively. The shifts upon coordination, if any, appear to be small and are upward; q, r, y, t, u, and x are found in the ranges 1099–1095, 688–687, 521–497, 450–416, 275–255, and

(11) Cotton, F. A.; Mester, Z. C.; Webb, T. R. *Acta Crystallogr., Sect. B: Struct. Crystallogr. Cryst. Chem.* **1974**, *30*, 2768.

(12) Whiffen, D. H. *J. Chem. Soc.* **1956**, 1350.

Table IV. Wavenumbers/cm⁻¹ of Bands Observed in the Resonance Raman Spectrum^a of [Rh₂(O₂CCD₃)₄(PPh₃)₂] at ca. 80 K

| $\tilde{\nu}$ | assignt | $\tilde{\nu}$ | assignt |
|---------------|------------------------------|---------------|---|
| 287 vs | $\nu_1, \nu(\text{Rh-Rh})$ | 1072 vw | d $\beta(\text{C-H})$ |
| 307 w | $\nu(\text{Rh-O})$ | 1100 w | q X-sens |
| 325 m | $\nu_2, \nu(\text{Rh-O})$ | 1133 vw | $\nu_1 + \nu_2 + \nu_3$ |
| 406 vw | w $\phi(\text{C-C})$ | 1147 vw | $4\nu_1$ |
| 421 vw | t X-sens | 1157 vw | c $\beta(\text{C-H})$ |
| 439 vw | | 1169 vw | |
| 449 vw | | 1186 vw | $3\nu_1 + \nu_2$ or a $\beta(\text{C-H})$ |
| 456 vw | | 1222 vw | $2\nu_1 + 2\nu_2$ |
| 520 m | ν_3, y X-sens | 1262 vw, sh | $\nu_1 + h$ $\gamma(\text{C-H})$ |
| 574 m | $2\nu_1$ | 1269 vw | e $\beta(\text{C-H})$ |
| 594 vw | $\nu_1 + 307$ | 1279 vw | |
| 612 m | $\nu_1 + \nu_2$ | 1287 vw | $\nu_1 + \text{p-ring}$ |
| 650 vw | $2\nu_2$ | 1326 vw | $\nu_1 + 2\nu_3$ or $\nu_2 + \text{p-ring}$ |
| 687 vw | r X-sens | 1387 vw | $\nu_1 + q$ X-sens |
| 692 vw | | 1424 vw, br | $\nu_2 + q$ X-sens |
| 697 vw | | 1433 vw | $5\nu_1$ |
| 707 vw | $\delta(\text{OCO})$ | 1471 vw | $4\nu_1 + \nu_2$ |
| 745 vw | f $\gamma(\text{C-H})$ | 1481 vw | m $\nu(\text{C-C})$ |
| 807 w | $\nu_1 + \nu_3$ | 1510 vw, br | $3\nu_1 + 2\nu_2$ |
| 845 vw | $\nu_2 + \nu_3$ | 1553 vw | |
| 860 w | $3\nu_1$ | 1571 vw | l $\nu(\text{C-C})$ |
| 882 vw | $2\nu_1 + 307$ | 1588 w | k $\nu(\text{C-C})$ |
| 899 w | $2\nu_1 + \nu_2$ | 1616 vw | $2\nu_1 + 2\nu_3$ |
| 936 vw | $\nu_1 + 2\nu_2$ | 1676 vw, br | $2\nu_1 + q$ X-sens |
| 976 vw | h $\gamma(\text{C-H})$ | 1712 vw, br | $\nu_1 + \nu_2 + q$ X-sens |
| 996 vw | $\nu_1 + \delta(\text{OCO})$ | 1760 vw | $5\nu_1 + \nu_2$ |
| 1001 w | p-ring | 1796 vw, br | $4\nu_1 + 2\nu_2$ |
| 1030 vw | b $\beta(\text{C-H})$ | 1876 vw | $\nu_1 + k$ $\nu(\text{C-C})$ |
| 1039 vw | $2\nu_3$ | 1914 vw | $\nu_2 + k$ $\nu(\text{C-C})$ |

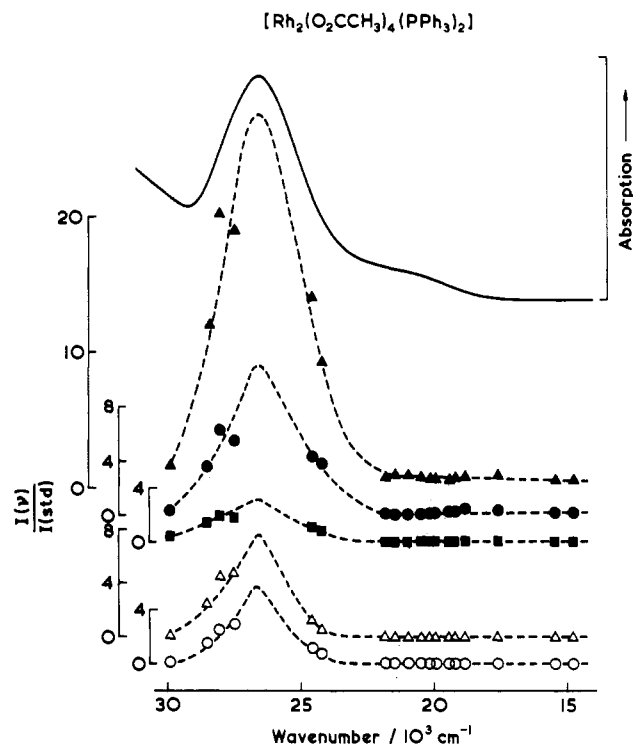
^a 356.4 nm excitation.

232–222 cm⁻¹, respectively, for Rh₂(O₂CCH₃)₄(PPh₃)₂. The smallness of the shifts on coordination is a reflection of the long Rh–P distances and hence weakness of these bonds.

In the resonance Raman spectrum $\nu(\text{Rh-Rh})$ forms combinations with $\nu(\text{Rh-O})$ and $\delta(\text{OCO})$ in a manner similar to that observed for Ru₂(O₂CCH₃)₄Cl₂,³ however, in addition, $\nu(\text{Rh-Rh})$ also forms combinations with the PPh₃ vibrations,² y X-sens, p-ring, q X-sens, and m and k $\nu(\text{C-C})$. The band assignments for

Table V. Wavenumbers/cm⁻¹ of Bands Observed in the Far-Infrared (660–40 cm⁻¹) Spectra of ¹⁶O, ¹⁸O, and CD₃ Derivatives of [Rh₂(O₂CCH₃)₄(PPh₃)₂] at ca. 80 K

| ¹⁶ O | | ¹⁸ O | | CD ₃ | |
|-----------------|---|-----------------|--|-----------------|---|
| $\tilde{\nu}$ | assignt | $\tilde{\nu}$ | assignt | $\tilde{\nu}$ | assignt |
| 627 w | out-of-plane $\rho_w(\text{COO})$ | 622 vw | out-of-plane $\rho_w(\text{COO})$ and s $\alpha(\text{C-C-C})$ | 619 vw | s $\alpha(\text{C-C-C})$ |
| 622 w | | 620 vw, sh | | 616 vw | |
| 619 vw | s $\alpha(\text{C-C-C})$ | 617 vw | in-plane $\rho_r(\text{COO})$ | 553 vw | in- and out-of-plane $\rho(\text{COO})$ |
| 616 vw | | 616 vw | | 548 vw | |
| 591 vw | in-plane $\rho_r(\text{COO})$ | 613 vw | y X-sens | 516 m | y X-sens |
| 587 vw | | 575 vw | | 504 m | |
| 515 m | y X-sens | 565 vw | y X-sens | 444 w | t X-sens |
| 504 m | | 515 m | | 436 w | |
| 497 m | t X-sens | 504 m | t X-sens | 405 vw | w $\phi(\text{C-C})$ |
| 494 w, sh | | 497 m | | 401 vw | |
| 444 w | w $\phi(\text{C-C})$ | 445 w | w $\phi(\text{C-C})$ | 373 w | $\nu(\text{Rh-O})$ |
| 436 w | | 436 w | | 366 w | |
| 416 vw | u X-sens | 405 vw | $\nu(\text{Rh-O})$ | 275 vw | u X-sens |
| 408 vw | | 396 vw | | 263 vw | |
| 405 vw | $\nu(\text{Rh-O})$ | 382 w | u X-sens | 230 vw | x X-sens |
| 400 vw | | 374 w | | 222 vw | |
| 396 vw | u X-sens | 315 vw | x X-sens | | |
| 385 w | | 255 vw | | | |
| 377 w | u X-sens | 231 vw | | | |
| 321 w | | 222 vw | | | |
| 275 vw | x X-sens | | | | |
| 264 vw | | | | | |
| 255 vw | $\delta(\text{O-Rh-O})$ or $\delta(\text{Rh-Rh-O})$ | | | | |
| 232 vw | | | | | |
| 222 vw | | | | | |
| 207 vw | | | | | |
| 197 vw | | | | | |
| 130 vw | | | | | |
| 124 vw | | | | | |
| 110 vw | | | | | |

**Figure 4.** Excitation profiles of ν_1 (▲), ν_2 (●), ν_3 (■), $2\nu_1$ (△), and $\nu_1 + \nu_2$ (○) for Rh₂(O₂CCH₃)₄(PPh₃)₂ at ca. 80 K, together with the transmission electronic spectrum at ca. 20 K.

the combinations are not necessarily unique; thus, for the ¹⁸O and CD₃ isotopomers, bands at 1329 and 1326 cm⁻¹, respectively, may be assigned to $\nu_1 + 2\nu_3$ or p-ring + ν_2 , although there is no such combination band observed for the ¹⁶O species. Band listings and assignments for Rh₂(O₂CCH₃)₄(PPh₃)₂ and the ¹⁸O and CD₃ isotopomers are given in Tables I–IV, respectively.

Table V contains band listings and assignments of the infrared spectra of Rh₂(O₂CCH₃)₄(PPh₃)₂ and the ¹⁸O and CD₃ iso-

omers in the range 700–40 cm⁻¹; full band listings and assignments (3,500–40 cm⁻¹) are included in the supplementary material (Tables VI–VIII). Assignments of the acetate group vibrations are taken from the data gathered for Rh₂(O₂CCH₃)₄,¹³ where the spectra are much simpler. In common with Mazo et al.,¹⁴ we make the assumption that the vibrations localized mainly in the acetate group show little dependence on the nature of the axial ligand, although many assignments, particularly those in the 1460–1400-cm⁻¹ region, remain tentative owing to overlap between such bands and ones due to PPh₃.

The observation of differing numbers of bands in both the infrared and resonance Raman spectra of Rh₂(O₂CCH₃)₄(PPh₃)₂ and its isotopomers is a consequence of two factors. First, many bands observed are very weak; hence, slight differences in signal-to-noise ratio between spectra affect the number of observables. Second, isotopic band shifts can reveal or obscure other bands.

Excitation profiles (EP's) have been constructed for the ν_1 , $\nu(\text{Rh-Rh})$, ν_2 , $\nu(\text{Rh-O})$, and ν_3 γ X-sens bands and also for the combination bands $2\nu_1$ and $\nu_1 + \nu_2$. These are shown in Figure 4. Quite clearly, the EP's of all the bands measured maximize within the contour of the 376-nm electronic absorption, although exact EP maxima were not achievable owing to the lack of a complete set of suitable exciting lines within this region. This absorption band has been assigned to the electric dipole allowed $\sigma \rightarrow \sigma^*$ transition of the Rh–Rh bond.¹⁵ Excitation within the contour of this band should lead primarily to a change in the metal–metal bond length, and hence, the resonance Raman spectrum would be expected to be dominated by a band progression in the metal–metal stretching vibration.^{16,17} This is the case here, with an overtone progression up to $4\nu_1$ being observed. However, very recently a different assignment has been proposed¹⁸ for the near-UV band of dirhodium tetraacetate complex ions of the sort $[\text{Rh}_2(\text{O}_2\text{CCH}_3)_4\text{L}_2]^{2-}$ (L = Cl⁻, Br⁻, I⁻), viz. that it is the $\sigma(\text{Rh-L}) \rightarrow \sigma^*(\text{Rh-Rh})$ transition. This assignment is strongly suggested for the above ions by the fact that the band maximum moves progressively toward the visible region in the wavenumber order Cl > Br > I, as would be expected for a LMCT transition. The problem with this assignment in the case of the complex Rh₂(O₂CCH₃)₄(PPh₃)₂ is that Raman spectra taken at resonance with the 376-nm transition might then have been expected to yield a considerably intensified $\nu(\text{Rh-P})$ band together with, depending on the extent of the Rh–P bond length change on excitation, a progression in $\nu(\text{Rh-P})$. Yet no band could be found that could

even be attributed to $\nu(\text{Rh-P})$ itself. Paradoxically, however, a number of X-sensitive modes act as enabling modes for readily observed progressions in ν_1 . The present results do not allow a firm distinction to be drawn between these alternative assignments^{15,18} for the 376-nm band except that it is z-polarized and undoubtedly involves a transition terminating in $\sigma^*(\text{Rh-Rh})$.

Further confirmation for the polarization comes from the depolarization ratio of the ν_1 band of Rh₂(O₂CCH₃)₄(PPh₃)₂. The polarizability tensor for a totally symmetric mode of a molecule of D_{4h} symmetry associated with a nondegenerate electronic transition will be dominated by its α_{zz} element on resonance. Consequently the ρ value of such a band will approach $1/3$ on-resonance, while any value between 0 and $3/4$ is expected off-resonance, depending on the relative sizes of the various tensor elements.^{16,17} In agreement with this, the depolarization ratio was found to be 0.34 when the band was excited with 363.8-nm radiation, confirming the axial (z) polarization of the electronic transition. Problems were encountered with sample decomposition due to the light-sensitive nature of the solutions. Consequently, the depolarization ratios were obtained by a technique of bracketing the measurements; i.e., first ρ_{\parallel} was recorded, followed by ρ_{\perp} , and then ρ_{\parallel} was measured again. The two ρ_{\parallel} values were then averaged. Obviously, this is not entirely satisfactory, and better results may be achieved by the development of a jet-flow system. Unfortunately, reliable depolarization ratios could not be obtained for ν_2 and ν_3 owing to their low band intensities; however, by virtue of the resonance enhancement of ν_2 and ν_3 , they are assumed to arise from totally symmetric fundamentals. It is significant, moreover, that independent work on the analogous SbPh₃ complex¹⁰ clearly indicates both ν_2 and ν_3 to be polarized. Attempts were also made to obtain off-resonance depolarization ratios, but surprisingly, even when 647.1-nm radiation was used, the sample decomposed.

Conclusions

The results obtained provide a firm basis for making vibrational band assignments for other dirhodium tetracarboxylates. The use of ¹⁸O and CD₃ derivatives has been necessary in order to distinguish between several of the key and close-lying skeletal modes. The principal progression-forming mode under resonance Raman conditions, ν_1 , is almost harmonic, with the anharmonicity constant $x_{11} \leq 0.2$ cm⁻¹; ν_1 acts as the progression-forming mode in at least 10 progressions, the enabling modes being other, presumably totally symmetric, fundamentals or overtones.

Acknowledgment. We thank the SERC and the ULIRS for financial support and Dr. S. P. Best for useful discussions.

Registry No. Rh₂(O₂CCH₃)₄(PPh₃)₂, 39773-08-5; Rh₂(¹⁸O₂CCH₃)₄(PPh₃)₂, 99829-59-1; Rh₂(O₂CCD₃)₄(PPh₃)₂, 99829-60-4; ¹⁸O, 14797-71-8; D₂, 7782-39-0.

Supplementary Material Available: Tables VI–VIII, containing full band listings and assignments for the infrared spectra of Rh₂(O₂CCH₃)₄(PPh₃)₂ and its ¹⁸O and CD₃ isotopomers (6 pages). Ordering information is given on any current masthead page.

- (13) Clark, R. J. H.; Hempleman, A. J. *Croat. Chem. Acta*, in press.
 (14) Mazo, G. Ya.; Baranovskii, I. B.; Shchelokov, R. N. *Russ. J. Inorg. Chem. (Engl. Transl.)* **1979**, *24*, 1855.
 (15) Sowa, T.; Kawamura, T.; Shida, T.; Yonezawa, T. *Inorg. Chem.* **1983**, *22*, 56.
 (16) Clark, R. J. H.; Stewart, B. *Struct. Bonding (Berlin)* **1979**, *36*, 1.
 (17) Clark, R. J. H.; Dines, T. J. *Angew. Chem., Int. Ed. Engl.* **1986**, *25*, 131.
 (18) Miskowski, V. M.; Dallinger, R. F.; Christoph, G. G.; Morris, D. E.; Spies, G. H.; Woodruff, W. H., *Inorg. Chem.* **1987**, *26*, 2127.